Spatial characterization of long-term hydrological change in the Arkavathy watershed adjacent to Bangalore, India

Gopal Penny[1], Veena Srinivasan[2], Iryna Dronova[3], Sharachchandra Lele[2], and Sally Thompson[1]

[1]Department of Civil and Environmental Engineering, University of California, Berkeley, Berkeley, California, USA
[2]Ashoka Trust for Research in Ecology and the Environment, Royal Enclave Sriramapura, Jakkur Post, Bangalore, Karnataka
[3]Department of Landscape Architecture and Environmental Planning, University of California, Berkeley, Berkeley, California, USA

Correspondence to: Gopal Penny (gopal@berkeley.edu)

Abstract. The complexity and heterogeneity of human water use over large spatial areas and decadal timescales can impede the understanding of hydrologic change, particularly in regions with sparse monitoring of the water cycle. In the Arkavathy watershed in south India, surface water inflows to major reservoirs decreased over a 40 year period during which urbanization, groundwater depletion, modification of the river network, and changes in agricultural practices also occurred. These multiple, interacting drivers combined with limited hydrological monitoring make attribution of the causes of diminishing water resources in the basin challenging and impede effective policy responses. To mitigate these challenges, we develop a novel, spatially distributed dataset to understand hydrologic change by characterizing trends in surface water and compare these trends with historical land use maps to assess human drivers of change. Using an automated classification approach with subpixel unmixing, we classified water surface area in nearly 1700 tanks in Landsat images from 1973 to 2010. The classification results compared well with a reference dataset of water surface area of tanks ($R^2 = 0.95$). We modeled water surface area of 42 clusters of tanks in a multiple regression on simple hydrological covariates and time, and found statistically significant trends, both positive and negative, in water surface area in different regions of the watershed. Wetting was found primarily downstream of Bangalore, likely due to increased urban effluents. Comparison of drying trends with land use indicated that trends in streamflow decline were most strongly associated with irrigated agriculture, suggesting that groundwater pumping for irrigation was a major driver of surface water change in this watershed. Disaggregating the watershed-scale hydrological response via remote sensing of surface water bodies over multiple decades yielded a spatially resolved characterization of hydrological change in an otherwise poorly monitored watershed. This approach presents an opportunity for understanding hydrological change in heavily managed watersheds where surface water bodies integrate upstream runoff and can be delineated using satellite imagery.

1 Introduction

Human water consumption is straining water resources worldwide (Vogel et al., 2015; Gleick, 2014; Wada et al., 2012; Lall et al., 2008), with developing nations particularly vulnerable to water scarcity (Vörösmarty et al., 2010). The causes of water scarcity are complex (Srinivasan et al., 2012) and in south India have been associated with urbanization (Srinivasan et al., 2013), groundwater depletion (Reddy, 2005), degradation of rainwater harvesting structures (Gunnell and Krishnamurthy, 2003), and interstate water disputes (Anand, 2004).

Effective management of water resources in south India requires a process-based understanding that relates changes in hydrology to the evolving human drivers of such change. Such human interventions in the water cycle often occur due to decisions made at local scales, and therefore exhibit considerable spatial heterogeneity when considered at larger scales. This is problematic in this region because most research linking human drivers to hydrologic responses focuses on either the local scale (Perrin et al., 2012; Van Meter et al., 2016), or regional to national scales (Gosain et al., 2011; Devineni et al., 2013; Tiwari et al., 2009). There is little research that addresses the emergent effects and heterogeneity of human-driven surface water change change across the watershed or basin scales at which management decisions must typically be made. The gap in scientific understanding at management-relevant scales is strongly associated with lack of data resolution at these scales, and forces water managers to make decisions without sufficient information about cause and effect within watersheds (Batchelor et al., 2003; Glendenning et al., 2012; Lele et al., 2013; Srinivasan et al., 2015).

The data scarcity that challenges understanding of human-driven hydrologic change in south India is a common challenge in hydrology and has been extensively explored through the lens of “predictions in ungauged basins” (PUB) over the past two decades (Bonell et al., 2006; Hrachowitz et al., 2013). The methodologies developed through the PUB initiative focused strongly on near-“natural” basins, where proxies for flow behavior (whether climatic, geographic or geomorphic) could be used to form a space in which to extrapolate flows observed in gauged basins to those in the ungauged site (Blöschl, 2013). Extending these techniques to heavily managed catchments presents numerous challenges, including the identification of suitable proxies to define the effects of human intervention and non-stationarity of the water cycle (Thompson et al., 2013). Given the complexity of these managed systems, hydrological reconstruction to infer or reproduce the history of hydrologic change can help identify the predominant processes that relate human water use and management with the hydrological response.

Here we present such a hydrologic reconstruction covering four decades of extensive hydrologic change in the Arkavathy watershed near Bangalore, India. Concern about water scarcity in the Arkavathy watershed has grown with the loss of historical monsoon-season river flow and reduced inflows to the TG Halli reservoir, which was the primary water supply reservoir for Bangalore between the 1930s and 1970s. These inflows have declined by nearly 80% since the late 1970s, a time period that also included groundwater depletion and loss of storage in surface reservoirs. Analysis by Srinivasan et al. (2015) showed that neither trends in precipitation nor evaporative demand could explain the observed changes in river flow. Instead, reductions in river channel flow were probably caused by human drivers of change such as expansion of *Eucalyptus* plantations, groundwater depletion associated with irrigated agriculture, and the construction of in-stream check dams (Srinivasan et al., 2015).

Groundwater irrigation grew in popularity in India in the 1960s (Briscoe and Malik, 2006), supplanting tank irrigation in south India in the following decades with the widespread adoption of borewells for groundwater pumping (Janakarajan, 1993a). Groundwater is now the dominant source of irrigation water in the Arkavathy watershed (Lele et al., 2013; Srinivasan et al., 2015). The availability of year-round reliable water supplies led to increases in the extent and intensity of agricultural production, and thus further demand for water. Replacement of traditional crops with *Eucalyptus* plantations, and population growth and urbanization around the periphery of Bangalore, the road network, and other urban hubs have also likely increased water demand. As villages and farmers became more reliant on groundwater, they attempted to augment groundwater recharge by constructing hundreds, if not thousands, of in-stream check dams which impound a portion of streamflow which is then removed from the channel via groundwater recharge or evaporation (Srinivasan et al., 2015). These decentralized land and water management decisions are spatially heterogeneous and characterizing their effects on surface water is hindered by the lack of hydrological records in the Arkavathy. However, spatially explicit characterization of variations in these drivers and hydrological change across the basin could offer a basis for drawing conclusions about the likely causes of change, thus assisting in the development of management approaches. To date, such analysis has been limited to anecdotal stakeholder accounts (Lele et al., 2013).

Our reconstruction relies on developing a history of change in post-monsoon season storage in widely distributed surface rainwater harvesting structures known as tanks (Vaidyanathan et al., 2001; Van Meter et al., 2014). Agriculture in south India was historically sustained by a series of reservoirs known collectively as the “cascading irrigation tank system”. Nearly 1700 tanks have been constructed in the Arkavathy watershed. Tanks typically consist of a long, shallow dam bund constructed across a river to harvest surface runoff during the monsoon and supply irrigation water during the dry season. The bund impedes streamflow until the tank fills, overflows, and “cascades” into downstream tanks. Although the dam bunds remain in place, village-level water managers report that the tanks rarely fill up and overflow in large portions of the Arkavathy (ATREE et al., 2015), similar to other watersheds in south India (Janakarajan, 1993b; Gunnell and Krishnamurthy, 2003; Kumar et al., 2016). This decline of tank water is a cause of concern in the Arkavathy and much of the region, and multiple efforts have been initiated to rejuvenate tanks, often without clear understanding of the drivers of degradation of the system (Kumar et al., 2016; Srinivasan et al., 2015).

Because the tanks are directly connected to surface flow in the river channel network, their surface area provides a proxy for surface flow generation over the upstream catchment area. *In situ* measurements of tank water storage have been successfully used to calibrate and validate hydrological models in Andhra Pradesh (Perrin et al., 2012) and Tamil Nadu (Van Meter et al., 2016). Other studies in south India (Mialhe et al., 2008), the USA (Halabisky et al., 2016), Africa (Meigh, 1995; Liebe et al., 2005; Sawunyama et al., 2006; Liebe et al., 2009; Gardelle et al., 2010) and South America (Rodrigues et al., 2012) also use surface water bodies as aggregators of streamflow.

Hydrological changes in the Arkavathy watershed should be apparent in historical satellite imagery, as the period of reported hydrological change in the Arkavathy (from the late 1970s onwards) coincides with the initial image collection by Landsat satellites in 1972. We develop an automated approach for estimating surface water area in tanks in the Arkavathy watershed using Landsat imagery and apply this approach to reconstruct a timeseries of water extent in tanks from 1973 to 2010. We use this dataset to identify temporal trends in water extent, hypothesizing that these trends reflect long-term hydrological changes induced by human activity. Specifically, we predict that areas with streamflow decline will correspond to agricultural land use associated with groundwater decline, either through groundwater irrigation or groundwater mining by *Eucalyptus* plantations. We conclude by comparing the temporal trends of streamflow against land use profiles developed by Lele and Sowmyashree M.V. (2016) as an initial estimate of competing influences of different land use practices on water resources throughout the Arkavathy watershed.

2 Methods

2.1 Study site

The Arkavathy watershed spans 4,253 km^2 on the western edge of the city of Bangalore in Karnataka, south India (Fig. 1). It has a monsoonal climate, with the rainy season lasting from June to November, relatively stable daily maximum temperature of 27°C, and mean annual rainfall of 830 mm. Temperature peaks near the end of dry season in April around 34°C, before pre-monsoon rainfall arrives sporadically in April and May. The river is gauged at TG Halli reservoir (Location 2, Fig. 1b) and upstream of Harobele reservoir (Location 5, Fig. 1b).

The watershed contains a mix of urban, natural and agricultural land uses. Agricultural land can be divided into rainfed grain crops, irrigated vegetable crops, *Eucalyptus* plantations, and other irrigated tree plantations (e.g., areca nut). Most present-day irrigation water in the Arkavathy is sourced from a deep, fractured rock aquifer. Irrigation from tanks is now significant in only a few locations, mostly located downstream of Bangalore. The city of Bangalore imports water from the regional Cauvery river and returns some urban wastewater to the Arkavathy system. Although many tanks are no longer in use, the tank structures remain intact and continue to capture surface water flows.

2.2 Remote-sensing images and supplementary data

Tracking water storage in the tanks at monthly or higher temporal resolution would be desirable, but is precluded because remotely sensed images from the monsoon season often contain large areas of cloud cover. This analysis therefore focuses on post monsoon images from the months of December and January. The highly seasonal monsoonal climate in south India means that end-of-monsoon tank water storage can be attributed primarily to the magnitude of streamflow filling the tank during monsoon season, allowing tank water storage to be used as a proxy for cumulative streamflow, minus any evaporation, drainage or extraction losses. Although these losses do occur, they can be accounted for during subsequent trend analysis.

We selected 48 Landsat images for classification, including 18 acceptable post-monsoon images from 1973 to 2010 for analyzing long-term hydrological trends (see Supplementary Material, Fig. S1 and Table S1 for dates). The 2014 Landsat imagery was used for remote-sensing validation and dry-season analysis, but was not included in the 1973–2010 study period. Most images were downloaded from Earth Explorer (earthexplorer.usgs.gov), except for five images from 1986 through 1993, which were purchased from the National Remote Sensing Centre (NRSC, nrsc.gov.in). An image from the Land Imagery Scan Sensor (LISS-IV) were also purchased from NRSC and used for accuracy assessment. A shapefile of tank boundaries was obtained from the Karnataka State Remote Sensing Application Centre (KSRSAC, karnataka.gov.in/ksrsac) to aid in classification of water bodies. Topographic maps completed in the 1970s by the Survey of India (surveyofindia.gov.in) were manually georeferenced and used to verify tank boundaries at the beginning of the study period. Other supplementary datasets were obtained from NASA Reverb (reverb.echo.nasa.gov) and Karnataka State Natural Disaster Monitoring Centre (KSNDMC) as listed in Table 1.

NRSC images were manually georeferenced using reference points from the higher-resolution LISS image, with root mean squared error (RMSE) less than 0.5 pixels in all images. All Landsat images were cropped to the extent of the Arkavathy

Dataset	Date	Resolution	Source
Landsat images	1973–2010 & 2014	30 m	USGS & NRSC
LISS IV image	2014	5 m	NRSC
Land use map	2001	30 m	KSRSAC
Tank boundaries	-	-	KSRSAC
Topographic maps	1970s	-	Survey of India
Aster DEM	-	30 m	NASA Reverb
Daily Precipitation (62 stations)	1972–2010	0.69 10km2	KSNDMC

Table 1. Data sources used in this paper.

watershed and converted to top-of-atmosphere (TOA) reflectance (Chander et al., 2009), which was used for training and classification of all images. Landsat 7 ETM+ scenes acquired after May 31, 2003 contained gaps due to a failure of the Scan Line Corrector (SLC) (Scaramuzza et al., 2005). Although gap-filling techniques for the SLC error generally use successive images to fill missing pixels (e.g., Chen et al., 2011), we used a single-image gap-filling approach because of the inherent temporal variability of tank water extent. We used pixels along the edge of the gap to fill missing pixels similar to Catts et al. (1985) but instead of interpolation, which would cause spectral homogenization in missing pixels, we repeated edge pixels towards the center of the gaps using using successive grayscale dilation.

We used cloud-free images where possible, but in some years the only viable post-monsoon image contained some cloud cover. Cloud shadows were particularly troublesome because the spectral reflectance of land in a cloud shadow was often similar to that of water. We applied the *fmask* algorithm (Zhu and Woodcock, 2012) to identify clouds and cloud shadows, making minor modifications to improve the method for the Bangalore region as follows: (i) we included the filters from the automatic cloud cover assessment algorithm (ACCA, Irish, 2000) when determining the potential cloud pixels, which reduced false positives for clouds in urban areas, and (ii) we removed clouds whose height (determined with *fmask*) was an outlier. This approach was possible because the topography was relatively flat and the selected images contained only cumulus clouds which exhibit relatively consistent base height at the lifting condensation level (Craven et al., 2002). Outliers were determined as clouds with a height less than $H_{25} - 1.5(H_{75} - H_{25})$ or greater than $H_{75} + 1.5(H_{75} - H_{25})$ where H_{25} and H_{75} are the first and third quartiles of cloud height and $H_{75} - H_{25}$ is the interquartile range. This procedure helped prevent erroneous classification of cold, white land pixels as clouds and limited the potential for erroneous classification of water bodies as shadows.

2.3 Classification method

The tank water classification method relied on separating pixels containing water from pixels containing land in a spatial region defined by the mapped tank boundaries. Water stored in tanks in the Arkavathy watershed varied from clear (with low reflectance in all Landsat reflectance bands) to turbid (more reflective in the visible (Moore, 1980) and NIR bands (Whitlock et al., 1981)). Turbid water exhibited its highest reflectance in the red band due to the red soils in the Arkavathy watershed (Novo et al., 1989) (see Figure 2).

Land cover surrounding wetted areas of tanks included vegetation, bare soil, and built-up urban land. We grouped these classes into a single land class, which was characterized by high reflectance in the NIR band and lower reflectance in visible bands (McFeeters, 1996). These characteristics primarily distinguish land from water in the Arkavathy, which has low reflectance in the NIR band and either low reflectance in the green band (clear water) or high reflectance in the red band (turbid water).

We developed an automated classification algorithm that distinguished areas of clear water and turbid water from land in each pixel, allowing rapid and consistent classification approach across images and Landsat sensors. We used a two-stage approach for estimating water extent in tanks. First, pixels having definitive spectral properties of water were identified and classified as “apparent” water pixels. Second, spectral unmixing was used to estimate the water fraction in all pixels within 60 m of any apparent water pixels. A conceptual representation of this algorithm is provided in Figure 3, and the steps described below are cross referenced to the numbered panels in the figure.

The only user input to the classification algorithm for each scene was to select a reservoir containing clear water with which to train the image (Fig. 3, step 1). The Normalized Difference Water Index by McFeeters (1996), NDWI = (green - NIR) / (green + NIR), reveals a clear distinction between land and water pixels. In each image, we divided pixels within the training reservoir (or a rectangular window of pixels around the training reservoir if the reservoir was mostly full) into water or land classes using Otsu’s method (Otsu, 1979), which clusters grayscale pixels into two classes by minimizing the within-class variance. The water and land pixels at the training reservoir were used to calculate the spectral means of land pixels and clear water pixels (step 2). The minimum NDWI of water pixels at the training reservoir (step 3a) was used as a threshold to create a mask of apparent clear water for the entire scene (step 3b) which was then dilated using a 5x5 square kernel (a 3x3 kernel for MSS scenes). All pixels within the dilated mask were transformed to a single component, $\hat{x}$, parallel to the transect between the spectral means of clear water and land in the 2-dimensional space of NIR and green reflectance (step 3c). Pixels falling between the $\hat{x}$ means of clear water and land were assigned a clear water fraction. Clear water fraction was set to 1 in pixels at or below the clear water $\hat{x}$ mean, and linearly decreased to 0 for pixels at or above the land $\hat{x}$ mean.

A similar procedure of masking, dilating, and unmixing was performed for turbid water, with minor changes. The criteria for apparent turbid water pixels were determined from land pixels near the training reservoir as the 98th percentile of red reflectance and the 98th percentile of NDWI (step 4a), provided that red reflectance was greater than NIR reflectance. Pixels meeting these criteria were included in the turbid water mask and dilated to include the surrounding area (step 4b). Spectral unmixing was conducted similarly to clear water, except the component for unmixing, $\hat{y}$, was taken along the transect between the spectral means of turbid water and land in the NIR-red space (step 4c). Finally, the water area in each pixel was taken as the higher value of clear water area and turbid water area (step 5). Tank water extent was calculated as the sum of water area of all pixels within two pixels of the mapped tank boundary (step 6).

We did not estimate the area of water in any tank that was flagged for the following quality concern criteria: (i) spatial overlap or adjacency of dry tank boundary or wetted tank area with clouds or cloud shadows, (ii) spatial overlap of greater than

25% of dry or wet tank area with missing pixels due to the SLC error in Landsat 7 images, or (iii) greater than 25% spatial overlap of dry or wet tank area with the edge of the scene from MSS images (step 7). In each of these cases, the tank area was recorded as “NA”.

Remote sensing and spatial processing were scripted in R (R Core Team, 2016) using the raster (Hijmans, 2015), rgeos (Bivand and Rundel, 2016), sp (Pebesma and Bivand, 2005), and rgdal (Bivand et al., 2016) packages, as well as ggplot (Wickham, 2009) for plotting. Watershed delineation and extraction of the cascading tank network were completed in GRASS GIS (GRASS Development Team, 2016).

2.4 Validation of classification method

To validate the classification results, we used a 5 m resolution LISS IV satellite image from 26 February 2014 to compare with a classified Landsat image from 27 February 2014. The LISS IV image was classified in ENVI software (Harris Geospatial Solutions Inc.) using support vector machine (SVM) classification with four land classes and four water classes. After classification, the water classes were merged into a single water class and resampled to the resolution of Landsat so that the resulting grayscale classification contained a water fraction in the range [0,1] for each pixel.

We compared the Landsat results with the results from the reference (LISS) classification at the pixel scale and tank scale, ignoring tanks in which there were obvious differences due to the incongruous image capture dates (e.g., cloud cover). At the pixel level, a traditional confusion matrix is inappropriate for continuous classification data (Congalton and Green, 2009). Thus, we evaluated the error (Landsat water fraction minus reference water fraction) in all pixels within tanks by binning the pixel error into categories representing under-classified (-1 to -0.2), correct (-0.2 to 0.2) and over-classified (0.2 to 1). We further separated pixels into groups by binning the producer (reference) water fraction and user (Landsat) water fraction. We calculated producer’s and user’s accuracy for each water fraction bin to form both a producer error matrix and consumer error matrix (see Sect. 3.1).

We also used Digital Globe imagery available from Google Earth (Google Earth, 2016) to assess the validity of the classification in normal and wet precipitation years during the study period. Given the limited availability of these images, we were unable to find a dry-year image within the study period that was suitable for comparison with a mostly cloud-free Landsat image. We manually delineated 18 tanks in the normal year (2009) and 34 tanks in wet years (2004 and 2005), and compared the manual delineation with classification of Landsat images from the same time period using a linear regression.

2.5 Statistical model for long-term hydrological change

We used a statistical modeling approach to identify long-term trends in tank water extent that could not be explained by readily available hydrological covariates (e.g., precipitation). We account for the effect of such explanatory variables in the model and posit that the remaining temporal trend in surface water extent indicates long-term hydrological changes induced by human activity. In the model, we exclude reservoirs, which are more likely to release water to users or downstream, and complicate the relationship between streamflow and reservoir water storage.

Because the timeseries for individual tanks were relatively short and contained many dry tanks, the dependent variable in the model was a spatially aggregated measure of water area in all tanks within a “tank cluster”. We divided the watershed into 8 subwatersheds, which were further subdivided into hydrologically-connected tank cluster watersheds, hereafter referred to as tank clusters (Fig. 4). Each tank cluster contained at least 15 tanks having non-zero water extent in at least 4 post-monsoon images. Tank clusters within each subwatershed were assumed to function as hydrologically similar units, with the only difference being the temporal trend in water extent over time.

Some tanks were constructed during the study period and were manually identified by examining the classification results of the largest 10 tanks in each cluster and verified using the Survey of India topographic maps. For these “new” tanks, we removed the tank (set the water extent to NA) in all scenes prior to the construction of the tank, unless there was a downstream tank within the same cluster, in which case the original classification (no water) was retained.

In an exploratory analysis we found that total surface water extent across the whole Arkavathy watershed was most strongly related to precipitation metrics computed from September 1, the approximate onset of the northeast monsoon, to the date of Landsat image acquisition. We anticipated that tank storage would respond to total seasonal precipitation as well as intense precipitation, which could lead to infiltration excess runoff. Because we only had access to daily precipitation data, we could not directly calculate precipitation intensity, and use the average depth of large storms (>10 mm/day) an alternative metric that would correlated with extreme rainfall.

For each post-monsoon Landsat scene, we calculated these metrics at up to 62 rain gauges reporting daily rainfall, omitting gauges in which the period of record excluded the monsoon year for the Landsat image. We spatially interpolated the rainfall metrics throughout the entire watershed using the inverse distance squared method, and calculated the spatial average for each tank cluster.

We exclusively used images that were taken early in the dry season (December or January), but we anticipated that there would be a relationship between the time that the image was taken and the wetted tank area, due to evaporative and drainage losses of water from the tanks. We incorporated a linear loss term using dry season days (DSD) as a covariate in the model, approximated as the number of days after December 1. To check the suitability of this assumption, we classified an additional 27 dry season Landsat images, and estimated the rate of decline of tank cluster water extent for years with at least two dry season images via linear regression. The nonparametric Mann–Kendall test was used to determine if there had been a change in dry season water losses over time, and showed that in only two subwatersheds, the Hesaraghatta and TG Halli East, the trends were significantly different from zero (i.e., the 95% bootstrap confidence intervals of the Mann–Kendall statistic excluded zero) (see Fig. S9). Presumably the trend in these two subwatersheds relates to the shift from tank irrigation to groundwater irrigation during the study period.

To understand the effects of carryover storage in tanks between years we developed a timeseries of tank water extent throughout the dry season of 2014 (chosen largely for image availability through the dry season). We confirmed that at the start of the 2014 monsoon, half of the tank clusters contained $\leq 25\%$ of 2013 post-monsoon storage. More than 75% of tank clusters contained $\leq 50\%$ of 2013 post-monsoon storage. Tank clusters with the highest carryover storage were found in urban subwatersheds or hilly sub watersheds at the southern part of the Arkavathy watershed. We were unable to consider any wet-season dynamics over the study period because of persistent cloud cover during monsoon season, which prohibits land-cover classification of most of these images.

We used a multivariate regression with interactions between continuous covariates and categorical variables (e.g., see Jaccard et al., 1990; Cohen et al., 2003) to estimate temporal trends in the different regions throughout the Arkavathy watershed. The covariates total precipitation, extreme precipitation, and tank water loss were modeled as fixed effects which interact with the subwatersheds. In other words, the response of the stored water area to these variables was allowed to vary for each subwatershed, but was assumed to be consistent for the tank clusters within the subwatershed. The model can be written as the following:

$$A_{cluster,ij} = C_0 + C_{1,k}P_{total,ij} + C_{2,k}P_{extreme,ij} + C_{3,k}DSD_i + B_{1,j}Year_i + e_{ij} \quad (1)$$

The subscripts refer to the Landsat scene (i), tank clusters (j), and subwatersheds (k). Other than the intercept (C_0), the fixed effects differ for each subwatershed ($C_{1,k}$, $C_{2,k}$, and $C_{3,k}$) or tank cluster ($B_{1,j}$). The model includes total precipitation depth (P_{total}) and the average depth ($P_{extreme}$) of large storms (>10 mm/day) as explanatory variables, calculated from September 1 through the date of the image. The errors for each observation are included as e_{ij}. The dependent variable ($A_{cluster,ij}$) is the normalized cluster area, where the cluster water extent of the scene is divided by the total maximum water extent of all tanks that were not removed from the scene. As a quality control measure, this area was set to NA for a given cluster and scene if more than 30% of the total tank area in the cluster was removed, either in classification (due to clouds or missing Landsat pixels) or in the assessment of tanks constructed during the study period. All covariates were centered by subtracting the mean before being input into the model. The primary result of interest is the value of the time trend for each cluster, $B_{1,j}$, which is the temporal trend in total tank water storage over time (as a percent change over time), after controlling for a stationary relationship between tankw water storage and the covariates (P_{total}, $P_{extreme}$, DSD). In the six subwatersheds where there is no change in the effect of dry season water losses, we interpret $B_{1,j}$ as a change in the relationship between rainfall and streamflow. In the two subwatersheds where we detect a change in the effect of dry season water loss on tank storage, $B_{1,j}$ captures the combined effect of hydrological change and dry-season tank water losses.

2.6 Linear regression of hydrological change and land use

We used four land use maps of the TG Halli watershed, encompassing the three subwatersheds upstream of the TG Halli reservoir (TG Halli East, Kumudavathy, and Hesaraghatta), developed for 1973-74, 1991-92, 2001-02, and 2013-14 (Lele and Sowmyashree M.V., 2016). The maps differentiate agricultural land use classes into rainfed crops, irrigated agriculture, and *Eucalyptus* plantations. Irrigated agriculture in this region is supplied almost exclusively by groundwater, allowing us to test whether groundwater irrigated agriculture, increased water utilization by *Eucalyptus* plantations (Srinivasan et al., 2015), both, or neither, are associated with the trends in surface flows.

In the early 1970s, rainfed agriculture was the primary land use in the TG Halli watershed. Over the study period, many farmers adopted groundwater irrigation and others converted their fields to *Eucalyptus* plantations, which have the potential to mine shallow groundwater or to significantly reduce deep recharge. These land use changes have the potential to reduce surface water flows by depleting subsurface water availability and baseflow over time. We therefore calculate the time-average land use fraction corresponding to irrigated crops ($A_{irrigated,avg}$) and *Eucalyptus* plantations ($A_{Eucs,avg}$) in each of the tank cluster watersheds, as a proxy for the cumulative effect on groundwater storage by that land use. We hypothesize that this time-averaged land use fraction correlates with the metric of hydrological change ($B_{1,j}$) developed in the statistical model. We test this hypothesis using a multivariate linear regression:

$$B_{1,j} = C_{Eucs} A_{Eucs,j} + C_{irrigated} A_{irrigated,j} \tag{2}$$

The coefficients, C_{Eucs} and $C_{irrigated}$, correspond to the sensitivity of hydrological change to time average *Eucalyptus* land cover and irrigated agriculture land cover, across all tank clusters. This analysis is not designed to directly infer causation, but rather to understand associations between streamflow decline and agricultural practices.

3 Results

3.1 Accuracy assessment

The Landsat classification yielded timeseries of surface water in each of the tanks throughout the watershed. The classification performed best for pixels that were fully dry or wet, when compared with the reference (LISS) classification in producer and consumer error matrices (Figure 5a). Producer accuracy was 84% for wet pixels and 99% for dry pixels, and because of the high number of dry pixels the overall accuracy was 98%. Pixels containing a mix of water and land (20–80% water) had lower producer accuracy (41–82%). Overall, the classification errors were unbiased and the histogram of classification errors (excluding pixels with zero error) was approximately normally distributed (Figure 5b).

The Landsat classification agreed well with the reference LISS classification at the tank scale, and accuracy improved with increasing tank size. A regression of Landsat extent versus reference extent (Figure 6) for tanks less than 25 hectares (27.8 pixels) had a slope of 0.98 and coefficient of determination (R^2) of 0.95. When all tanks and reservoirs were included, the regression line had a slope of 1.02 and coefficient of determination of 0.99. Over 99% of dry tanks were correctly classified as dry, but error was considerably large for small tanks with non-zero water extent less than 2.5 ha (2.8 pixels), due to false positives in the reference classification as well as errors the Landsat classification. For tanks between 2.5 and 10 ha the classification performed considerably better. The mean absolute error increased as the extent of the water body increased, but mean percent error decreased with water body size.

Comparison of our automated Landsat classification similarly compared well with the Google Earth manual delineation of tanks in both normal years (R^2 = 0.97) and wet years (R^2 = 0.97) (see Fig. S6).

Although the time-trends in most tanks have not been reported as ground data, trends in water storage over time are widely known for some of the major reservoirs. The TG Halli and Hesaraghatta reservoirs declined from a peak storage in the 1970s to much lower contemporary storage. Large increases in water extent were observed in Manchanabele reservoir, which was constructed in 1993, and Harobele reservoir which was constructed in 2004. These anecdotal trends corroborate our findings for these specific structures.

3.2 Long-term trends in surface water

The multivariate analysis yielded both negative and positive values of $B_{1,j}$ (Table S2) revealing drying and wetting in different parts of the Arkavathy watershed, with statistically significant trends in 13 tank clusters. The model explained nearly 70% of the variation in tank cluster water extent (R^2 = 0.68). The effects (slopes) of both precipitation covariates were significant (the 95% confidence interval of the slope of the temporal trend excluded zero) in nearly all subwatersheds, and the effect of dry-season water loss was significant in the two subwatersheds that flow into TG Halli reservoir.

In the two subwatersheds flowing directly into the TG Halli reservoir, $B_{1,j}$ captured the combined effect of hydrological change (streamflow decline pushes $B_{1,j}$ in the negative direction) and dry-season tank water losses (lower tank losses pushes $B_{1,j}$ in a the positive direction). Where $B_{1,j}$ is negative in this area, the effect of hydrological change must exceed that of reduced tank water losses. We converted the units of $B_{1,j}$ to an areal rate of change over time per 10 km^2 of catchment area (Figure 7). In the three subwatersheds upstream of TG Halli reservoir, most tank clusters showed a drying trend. Tanks within Bangalore generally exhibited drying trends, and tanks at the city periphery and immediately downstream showed wetting trends. Other regions of the watershed exhibited mixed results in changing water extent, but none of the trends were statistically significant at the 95% confidence level.

3.3 Streamflow decline and agricultural practices

The regression of hydrological change on irrigated agriculture and *Eucalyptus* land use areas explained most of the variation in hydrological change (R^2 = 0.68) between tank clusters. The relationship between irrigated crops and hydrological change was statistically significant (95% confidence intervals of $C_{irrigated}$ excluded zero), while the relationship with *Eucalyptus* plantations was not statistically significant (Fig. 8).

4 Discussion

4.1 Long-term hydrological trends and human drivers of change

Our analysis confirms that tank water extent at the end of the monsoon season can be primarily attributed to the storage of monsoon season streamflow. Because tanks in the Arkavathy watershed rarely overflow today and there is little carry-over storage year to year, the volume of water in tanks provides an integrated measure of hydrological processes from the previous wet season. Using historical land use maps for the TG Halli watershed we can also make associations between variations in the observed streamflow decline and variations in human drivers of change.

We hypothesized that the declines in streamflow would correspond with agricultural practices associated with groundwater depletion. Although little data exists to describe historical decline of the water table, contemporary farmers typically have to drill new borewells to depths exceeding 100 m to reach any groundwater. If a loss of baseflow due to groundwater depletion and the disconnection of the water table from the stream channel is a primary driver of streamflow decline, we would expect the negative trends in streamflow to correspond with irrigated agriculture, which is supplied almost entirely by groundwater in the TG Halli watershed.

In the linear model relating streamflow changes to land use in the TG Halli watershed, the time-averaged irrigated crop land use area is a clearer and stronger predictor of declines in tank inflow than *Eucalyptus* land use. Moreover, other exploratory analyses showed that irrigated crop land-use is more correlated with streamflow decline ($R^2 = 0.68$) than rainfed crops ($R^2 = 0.5$) and all other land-use types ($R^2 < 0.38$). Areas retaining mostly rainfed crops exhibit less of a decline in streamflow, and the decline in streamflow is associated with areas with higher conversion of rainfed crops to irrigated crops. The finding that *Eucalyptus* plantations do not play a major role in streamflow decline is consistent with field experiments, which show that that *Eucalyptus* plantations tend to reduce infiltration capacity and therefore would increase infiltration excess runoff (Penny et al., 2015). There could be some relationship between *Eucalyptus* plantations and tank inflow decline, but if so it is secondary to that of irrigated crops.

Irrigated agriculture is also likely to contain relatively higher densities of check dams than other other land use types, given the desire to recharge diminished groundwater resources. In the absence of datasets describing the spatial distribution and hydrologic properties of check dams (or a viable way to develop such a dataset), our analysis is unable to separate the effect of loss of baseflow due to groundwater pumping from the in-stream losses due to check dams. Both processes likely play a role in observed hydrological changes. Recession analyses indicate that the loss of the shallow water table could plausibly explain the observed magnitude of streamflow declines (Srinivasan et al., 2015), and check dams exacerbate the loss of streamflow by converting water in the stream channel to groundwater recharge (Jeremiah et al., 2014).

The highest streamflow decline occurs in the northernmost regions of the Arkavathy where elevation is higher than other areas of the watershed. Although it may appear that the pattern of decline could be related to upstream-downstream processes and the presence or absence of irrigation return flows (Van Meter et al., 2016, e.g., see), we are doubtful that this effect is important in the Arkavathy today. Indirect evidence (e.g., surveys) indicates that the water table is hundreds of meters below the surface in northern parts of the Arkavathy watershed (Srinivasan et al., 2015). Furthermore, the relief in the watershed is only about 100 m over a distance of 50 km in the TG Halli watershed, meaning that system-wide return flows connecting upstream to downstream are unlikely.

Urbanization can have a wetting effect on downstream tanks, due to increases in impervious surfaces, the fallowing of agricultural land in anticipation of urbanization, and reduced consumptive water use. There is also a non-local effect in that increased urban water use produces increased urban effluent, which is discharged to the surface channel network where it can contribute to increases in tank water storage downstream. The observed increases make sense given Bangalore's imports from the Cauvery river have increased substantially from 185 million liters per day (MLD) in 1974 to 1350 MLD currently (BWSSB, 2017), Additionally, as the city has grown, groundwater pumping for urban areas has also increased to an estimated 600 MLD (Lele et al., 2013). About 40% of Bangalore's sewage of 1400 MLD flows to Byramangala reservoir (Jamwal et al., 2015). This has contributed to additional inflows to Byramangala reservoir and more irrigated agriculture directly downstream of the reservoir. Tanks within urban areas can also exhibit drying trends. For instance, tanks may be encroached upon as residential areas expand. Additional urban wastewater inflow can lead to expansion of algae blooms covering the tank water surface, which can appear as a "drying" of the tank in this analysis.

4.2 Assessing the classification and model uncertainty

The classification of small tanks in the Arkavathy watershed poses challenges associated with harmonization of different Landsat sensors and the variability in the spectral properties of “wet” tanks due to variations in water quality and vegetation extent. The classification tends to overestimate the amount of water in dry pixels and underestimate the amount of water in wet and mixed pixels. Because our classification scheme is designed to avoid bias between images taken with different Landsat sensors, we likely sacrifice some precision with sensors from Landsat missions 5–8.

Because these pixels lie at the boundary of the wetted tank area, classification error would be sensitive to geo-registration error in one or both of the images. Error could also arise from our specification that water pixels must lie within 60 m of clearly identifiable water bodies, or the assumptions made during spectral unmixing. Although the classification scheme accounted for only two classes, the spectral properties of the land class varied among dry soil, wet soil, sparse vegetation, and irrigated agriculture. Classification of water was complicated by vegetation in tanks, varying degrees of turbidity, and algae blooms in tanks with considerable wastewater inflow.

Errors at the pixel and tank scales are likely unavoidable given the spectral heterogeneity of both land and water pixels. In particular, tanks containing water of variable turbidity, excessive vegetation, or algae blooms are prone to classification errors. Because pixel-scale errors are unbiased, accuracy at the tank scale improves as tank size increases. Error is further mitigated by grouping tanks into clusters in the statistical model.

The uncertainty of the classification ($R^2 = 0.99$ when all water bodies are included) is small compared with the uncertainty of the statistical model ($R^2 = 0.68$). Although the results of our statistical model imply a non-trivial amount of unexplained variation, Gardelle et al. (2010) reported similar performance ($R^2 = 0.78$) for a model relating precipitation and water extent in a single lake, and noted that the correlation was valid only for a nine-year subset of the five-decade study period. The sources of uncertainty include the complex hydrological processes that relate precipitation, streamflow, and tank water storage, as well as the nonlinear and heterogeneous relationship between water extent and water storage and the non-stationary behavior of dry-season losses in the two northermost watersheds. Given this uncertainty, results of our analysis are reasonable given the simplicity of the model and the complexity and heterogeneity of the watershed hydrological response.

5 Conclusions

The Arkavathy watershed embodies many of the water security challenges confronting southern India. With data limitations hampering the characterization of changing water supplies in the basin, remote sensing tools provide insights into the history and spatial pattern of change in water availability. We were able to take advantage of a pre-existing "sensing network" provided by the irrigation tank system throughout the Arkavathy watershed. The high number of tanks in this watershed allowed for a comparison of hydrological change with land use at spatial scales appropriate for a first-order analysis.

The analysis reveals that changes in surface water resources are not spatially homogeneous, but vary in their magnitude and sign among different regions of the basin. These differences appear to be associated with differing patterns of land use across the basin. A comparison of the hydrological trends with agricultural practices within the TG Halli watershed showed that streamflow decline is more closely associated with groundwater irrigated agriculture than other kinds of land use, including *Eucalyptus* plantations. Groundwater depletion appears to be an important driver of streamflow decline, likely because of the direct consequence of the disconnection of the water table from the stream channel as well as the indirect consequence of check dam construction in groundwater-depleted areas. Further investigation could attempt to attribute the cause of streamflow decline, either via a more sophisticated statistical analysis considering the many potential drivers of change or via a mechanistic model of catchment hydrologic functioning. Ideally such analysis would also separate the relative effects of loss of baseflow due to groundwater pumping and conversion of surface flows to groundwater recharge via check dams.

Surface networks of rainwater harvesting structures are employed in seasonal climates worldwide, whether in cascading tank systems in southern India and Sri Lanka, or hillslope farm dams in Australia (Callow and Smettem, 2009; Roohi and Webb, 2012), North-East Brazil (Lima Neto et al., 2011; Malveira et al., 2012; de Araújo and Medeiros, 2013; de Toledo et al., 2014), South Africa (Hughes and Mantel, 2010), the US Great Plains (Womack et al., 2012) and China (Xiankun, 2014; Xu et al., 2013). Capitalizing on these networks as proxy indicators of rainfall and streamflow variation, as in the Arkavathy, could prove a valuable approach to circumventing problems of data scarcity and characterizing changing hydrological conditions.

Acknowledgements. We thank the ATREE's EcoInformatics Lab for RS/GIS support, including M. Mariappan for help in procuring satellite imagery. Penny acknowledges support from the NSF Graduate Research Fellowship Program under Grant No. DGE 1106400, the NSF and USAID GROW Fellowship Program. Srinivasan and Lele acknowledges financial support for this research from Grant No. 107086-001 from the International Development Research Centre (IDRC), Canada. Thompson acknowledges NSF CNIC IIA-1427761 for support of ATREE-UC Berkeley collaborations.

References

Anand, P. B.: Water and Identity: An analysis of the Cauvery River water dispute., University of Bradford, pp. 1–41, http://hdl.handle.net/10454/2893, 2004.

ATREE, Srinivasan, V., and Lele, S.: Forum with traditional watermen (Neerghantis) in the upper Arkavathy sub-basin, 2015.

Batchelor, C., Rama Mohan Rao, M., and Manohar Rao, S.: Watershed development: A solution to water shortages in semi-arid India or part of the problem, Land Use and Water . . . , pp. 1–10, http://www.rainfedfarming.org/documents/Groundwater/luwrrpap.pdf, 2003.

Bivand, R. and Rundel, C.: rgeos: Interface to Geometry Engine - Open Source (GEOS), https://CRAN.R-project.org/package=rgeos, r package version 0.3-19, 2016.

Bivand, R., Keitt, T., and Rowlingson, B.: rgdal: Bindings for the Geospatial Data Abstraction Library, https://CRAN.R-project.org/package=rgdal, r package version 1.1-8, 2016.

Blöschl, G.: Runoff prediction in ungauged basins: synthesis across processes, places and scales, Cambridge University Press, 2013.

Bonell, M., McDonnell, J. J., Scatena, F., Seibert, J., Uhlenbrook, S., and Van Lanen, H. A.: HELPing FRIENDs in PUBs: charting a course for synergies within international water research programmes in gauged and ungauged basins, Hydrological Processes, 20, 1867–1874, 2006.

Briscoe, J. and Malik, R.: India's water economy: bracing for a turbulent future, Tech. Rep. 34750, World Bank, https://openknowledge.worldbank.org/handle/10986/7238, 2006.

BWSSB: About BWSSB (Bangalore Water Supply and Sewerage Board), https://bwssb.gov.in/content/about-bwssb-2, 2017.

Callow, J. N. and Smettem, K. R. J.: The effect of farm dams and constructed banks on hydrologic connectivity and runoff estimation in agricultural landscapes, Environmental Modelling & Software, 24, 959–968, 2009.

Catts, G., Khorram, S., Knight, A., and DeGloria, S.: Remote sensing of tidal chlorophyll-a variations in estuaries, International Journal of Remote Sensing, 6, 1685–1706, doi:10.1080/01431168508948318, 1985.

Chander, G., Markham, B. L., and Helder, D. L.: Summary of current radiometric calibration coefficients for Landsat MSS, TM, ETM+, and EO-1 ALI sensors, Remote Sensing of Environment, 113, 893–903, doi:10.1016/j.rse.2009.01.007, http://linkinghub.elsevier.com/retrieve/pii/S0034425709000169, 2009.

Chen, J., Zhu, X., Vogelmann, J. E., Gao, F., and Jin, S.: A simple and effective method for filling gaps in Landsat ETM+ SLC-off images, Remote Sensing of Environment, 115, 1053–1064, doi:10.1016/j.rse.2010.12.010, 2011.

Cohen, J., Cohen, P., West, S. G., and Aiken, L.: Applied Multiple Regression / Correlation Analysis for the Behavioral Sciences, vol. Third Edit, doi:10.2307/2064799, http://books.google.com/books?hl=de{&}lr={&}id=fuq94a8C0ioC{&}pgis=1, 2003.

Congalton, R. G. and Green, K.: Assessing the Accuracy of Remotely Sensed Data: Principles and Practices, vol. 2, CRC/Taylor & Francis Group, LLC, Boca Raton, London, New York, doi:10.1111/j.1477-9730.2010.00574_2.x, http://www.loc.gov/catdir/enhancements/fy0744/98029658-d.html, 2009.

Craven, J. P., Jewell, R. E., and Brooks, H. E.: Comparison between observed convective cloud-base heights and lifting condensation level for two different lifted parcels, Weather and Forecasting, 17, 885–890, doi:10.1175/1520-0434(2002)017<0885:CBOCCB>2.0.CO;2, 2002.

de Araújo, J. and Medeiros, P.: Impact of dense reservoir networks on water resources in semiarid environments, Australian Journal of Water Resources, 17, 87–100, 2013.

de Toledo, C. E., de Araújo, J. C., and de Almeida, C. L.: The use of remote-sensing techniques to monitor dense reservoir networks in the Brazilian semiarid region, International Journal of Remote Sensing, 35, 3683–3699, 2014.

Devineni, N., Perveen, S., and Lall, U.: Assessing chronic and climate-induced water risk through spatially distributed cumulative deficit measures: A new picture of water sustainability in India, Water Resources Research, 49, 2135–2145, doi:10.1002/wrcr.20184, 2013.

Gardelle, J., Hiernaux, P., Kergoat, L., and Grippa, M.: Less rain, more water in ponds: a remote sensing study of the dynamics of surface waters from 1950 to present in pastoral Sahel (Gourma region, Mali), Hydrology and Earth System Sciences, 14, 309–324, doi:10.5194/hess-14-309-2010, http://www.hydrol-earth-syst-sci.net/14/309/2010/, 2010.

Gleick, P.: The World's Water Volume 8, vol. 8, Island Press/Center for Resource Economics, Washington, DC, http://worldwater.org/water-data/, 2014.

Glendenning, C., van Ogtrop, F., a.K. Mishra, and Vervoort, R.: Balancing watershed and local scale impacts of rain water harvesting in India—A review, Agricultural Water Management, 107, 1–13, doi:10.1016/j.agwat.2012.01.011, http://linkinghub.elsevier.com/retrieve/pii/S0378377412000273, 2012.

Google Earth: version 7.1.7.2606. Karnataka, India, 2004-2009, approx. 13°00'N 77°30'E. DigitalGlobe 2016, http://www.earth.google.com, [accessed March, 2017], 2016.

Gosain, A., Rao, S., and Arora, A.: Climate change impact assessment of water resources of India, Current Science(Bangalore), http://www.currentscience.ac.in/Volumes/101/03/0356.pdf, 2011.

GRASS Development Team: Geographic Resources Analysis Support System (GRASS GIS) Software, Version 7.0, Open Source Geospatial Foundation, http://grass.osgeo.org, 2016.

Gunnell, Y. and Krishnamurthy, A.: Past and Present Status of Runoff Harvesting Systems in Dryland Peninsular India: A Critical Review, Ambio, 32, 320–323, doi:10.1579/0044-7447-32.4.320, http://www.bioone.org/doi/abs/10.1579/0044-7447(2003)032[0320:PAPSOR]2.0.CO;2, 2003.

Halabisky, M., Moskal, L. M., Gillespie, A., and Hannam, M.: Reconstructing semi-arid wetland surface water dynamics through spectral mixture analysis of a time series of Landsat satellite images (1984-2011), Remote Sensing of Environment, 177, 171–183, doi:10.1016/j.rse.2016.02.040, 2016.

Hijmans, R. J.: raster: Geographic Data Analysis and Modeling, https://CRAN.R-project.org/package=raster, r package version 2.5-2, 2015.

Hrachowitz, M., Savenije, H., Blöschl, G., McDonnell, J., Sivapalan, M., Pomeroy, J., Arheimer, B., Blume, T., Clark, M., Ehret, U., et al.: A decade of Predictions in Ungauged Basins (PUB)—a review, Hydrological sciences journal, 58, 1198–1255, 2013.

Hughes, D. and Mantel, S.: Estimating the uncertainty in simulating the impacts of small farm dams on streamflow regimes in South Africa, Hydrological Sciences Journal–Journal des Sciences Hydrologiques, 55, 578–592, 2010.

Irish, R. R.: Landsat 7 automatic cloud cover assessment, AeroSense 2000, 4049, 348–355, doi:10.1117/12.410358, http://proceedings.spiedigitallibrary.org/data/Conferences/SPIEP/35040/348{_}1.pdf, 2000.

Jaccard, J., Wan, C. K., and Turrisi, R.: The Detection and Interpretation of Interaction Effects Between Continuous Variables in Multiple Regression, Multivariate Behavioral Research, 25, 467–478, doi:10.1207/s15327906mbr2504_4, 1990.

Jamwal, P., Zuhail, T., Urs, P. R., and Srinivasan, V.: Contribution of sewage treatment to pollution abatement of urban streams, Current Science, 108, No 4,, 677–685, 2015.

Janakarajan, S.: In Search of Tanks : Some Hidden Facts, Economic and Political Weekly, 28, A53–A60, 1993a.

Janakarajan, S.: Economic and Social Implications of Groundwater Irrigation: Some Evidence from South India, Indian journal of agricultural economics, 48, 65–75, 1993b.

Jeremiah, K., Srinivasan, V., et al.: Evaporation Ponds or Recharge Structures? the Role of Check Dams in Arkavathy River Basin, India, in: AGU Fall Meeting Abstracts, vol. 1, p. 0854, 2014.

Kumar, M. D., Bassi, N., Kishan, K. S., Chattopadhyay, S., and Ganguly, A.: Rejuvenating Tanks in Telangana, Economic & Political Weekly, lI, 30–34, 2016.

Lall, U., Heikkila, T., Brown, C., and Siegfried, T.: Water in the 21st century: Defining the elements of global crises and potential solutions, Journal of International Affairs, 61, 1–17, http://water.columbia.edu/files/2011/11/LallSiegfried2008Water.pdf, 2008.

Lele, S. and Sowmyashree M.V.: Land use and land cover change in the Arkavathy basin, in: Adapting to Climate Change in Urbanising Watersheds: National Dissemination Workshop, edited by ATREE, New Delhi, 22-23 August, 2016.

Lele, S., Srinivasan, V., Jamwal, P., Thomas, B. K., Eswar, M., and Zuhail, T. M.: Water Management In Arkavathy Basin: A situational analysis, Tech. Rep. 1, Ashoka Trust for Research in Ecology and the Environment, Bengaluru, 2013.

Liebe, J., van de Giesen, N., and Andreini, M.: Estimation of small reservoir storage capacities in a semi-arid environment: A case study in the Upper East Region of Ghana, Physics and Chemistry of the Earth, 30, 448–454, doi:10.1016/j.pce.2005.06.011, http://linkinghub.elsevier.com/retrieve/pii/S1474706505000409, 2005.

Liebe, J. R., Van De Giesen, N., Andreini, M., Walter, M. T., and Steenhuis, T. S.: Determining watershed response in data poor environments with remotely sensed small reservoirs as runoff gauges, Water Resources Research, 45, W07 410, doi:10.1029/2008WR007369, http://www.agu.org/pubs/crossref/2009/2008WR007369.shtml, 2009.

Lima Neto, I. E., Wiegand, M. C., and de Araújo, J. C.: Sediment redistribution due to a dense reservoir network in a large semi-arid Brazilian basin, Hydrological Sciences Journal–Journal des Sciences Hydrologiques, 56, 319–333, 2011.

Malveira, V. T. C., de Araújo, J. C., and Güntner, A.: Hydrological Impact of a High-Density Reservoir Network in Semiarid Northeastern Brazil, Journal of Hydrologic Engineering, 17, 109–117, doi:10.1061/(ASCE)HE.1943-5584.0000404, 2012.

McFeeters, S. K.: The use of the Normalized Difference Water Index (NDWI) in the delineation of open water features, International Journal of Remote Sensing, 17, 1425–1432, doi:10.1080/01431169608948714, http://www.tandfonline.com/doi/abs/10.1080/01431169608948714, 1996.

Meigh, J.: The impact of small farm reservoirs on urban water supplies in Botswana, Natural Resources Forum, 19, 71–83, doi:10.1111/j.1477-8947.1995.tb00594.x, 1995.

Mialhe, F., Gunnell, Y., and Mering, C.: Synoptic assessment of water resource variability in reservoirs by remote sensing: General approach and application to the runoff harvesting systems of south India, Water Resources Research, 44, n/a–n/a, doi:10.1029/2007WR006065, http://doi.wiley.com/10.1029/2007WR006065, 2008.

Moore, G. K.: Satellite remote sensing of water turbidity / Sonde de télémesure par satellite de la turbidité de l'eau, Hydrological Sciences Bulletin, 25, 407–421, doi:10.1080/02626668009491950, http://www.tandfonline.com/doi/abs/10.1080/02626668009491950, 1980.

Novo, E., Hansom, J., and Curran, P.: The effect of viewing geometry and wavelength on the relationship between reflectance and suspended sediment concentration, International Journal of Remote Sensing, 10, 1357–1372, doi:10.1080/01431168908903973, http://www.tandfonline.com/doi/abs/10.1080/01431168908903973$\delimiter"026E30F$nhttp://www.tandfonline.com/doi/abs/10.1080/01431168908903973{#}.Uzro0leUTz8$\delimiter"026E30F$nhttp://www.tandfonline.com/doi/pdf/10.1080/01431168908903973, 1989.

Otsu, N.: A threshold selection method from gray-level histograms, IEEE Transactions on Systems, Man, and Cybernetics, 9, 62–66, doi:10.1109/TSMC.1979.4310076, http://web-ext.u-aizu.ac.jp/course/bmclass/documents/otsu1979.pdfhttp://ieeexplore.ieee.org/lpdocs/epic03/wrapper.htm?arnumber=4310076, 1979.

Pebesma, E. J. and Bivand, R. S.: Classes and methods for spatial data in R, R News, 5, 9–13, http://CRAN.R-project.org/doc/Rnews/, 2005.

Penny, G., Thompson, S., Srinivasan, V., Peschel, J., Young, S., Jeremiah, K., et al.: Streamflow generation in a drying catchment outside Bangalore, India, in: AGU Fall Meeting Abstracts, 2015.

Perrin, J., Ferrant, S., Massuel, S., Dewandel, B., Maréchal, J. C., Aulong, S., and Ahmed, S.: Assessing water availability in a semi-arid watershed of southern India using a semi-distributed model, Journal of Hydrology, 460-461, 143–155, doi:10.1016/j.jhydrol.2012.07.002, http://linkinghub.elsevier.com/retrieve/pii/S0022169412005598, 2012.

R Core Team: R: A Language and Environment for Statistical Computing, R Foundation for Statistical Computing, Vienna, Austria, https://www.R-project.org/, 2016.

Reddy, V. R.: Costs of resource depletion externalities: a study of groundwater overexploitation in Andhra Pradesh, India\n \n , Environment and Development Economics, 10, 533–556, doi:10.1017/S1355770X05002329, http://www.journals.cambridge.org/abstract{_}S1355770X05002329, 2005.

Rodrigues, L. N., Sano, E. E., Steenhuis, T. S., and Passo, D. P.: Estimation of small reservoir storage capacities with remote sensing in the Brazilian Savannah region, Water Resources Management, 26, 873–882, doi:10.1007/s11269-011-9941-8, http://link.springer.com/10.1007/s11269-011-9941-8, 2012.

Roohi, R. and Webb, J.: Landsat Image Based Temporal and Spatial Analysis of Farm Dams in Western Victoria., in: GSR, Citeseer, 2012.

Sawunyama, T., Senzanje, A., and Mhizha, A.: Estimation of small reservoir storage capacities in Limpopo River Basin using geographical information systems (GIS) and remotely sensed surface areas: Case of Mzingwane catchment, Physics and Chemistry of the Earth, 31, 935–943, doi:10.1016/j.pce.2006.08.008, http://linkinghub.elsevier.com/retrieve/pii/S1474706506001677, 2006.

Scaramuzza, P. L., Schmidt, G., Storey, J. C., and Barsi, J.: Landsat 7 Scan Line Corrector-Off Gap-Filled Product Gap-Filled Product Development Process, In Proceedings of Pecora, 16, 23–27, 2005.

Srinivasan, V., Lambin, E. F., Gorelick, S. M., Thompson, B. H., and Rozelle, S.: The nature and causes of the global water crisis: Syndromes from a meta-analysis of coupled human-water studies, Water Resources Research, 48, 1–16, doi:10.1029/2011WR011087, http://www.agu.org/pubs/crossref/2012/2011WR011087.shtml, 2012.

Srinivasan, V., Seto, K. C., Emerson, R., and Gorelick, S. M.: The impact of urbanization on water vulnerability: A coupled human-environment system approach for Chennai, India, Global Environmental Change, 23, 229–239, doi:10.1016/j.gloenvcha.2012.10.002, http://linkinghub.elsevier.com/retrieve/pii/S095937801200115X, 2013.

Srinivasan, V., Thompson, S., Madhyastha, K., Penny, G., Jeremiah, K., and Lele, S.: Why is the Arkavathy River drying? A multiple hypothesis approach in a data scarce region, Hydrology and Earth System Sciences Discussions, 12, 25–66, doi:10.5194/hessd-12-25-2015, http://www.hydrol-earth-syst-sci-discuss.net/12/25/2015/, 2015.

Thompson, S., Sivapalan, M., Harman, C., Srinivasan, V., Hipsey, M., Reed, P., Montanari, A., and Blöschl, G.: Developing predictive insight into changing water systems: use-inspired hydrologic science for the Anthropocene, Hydrology and Earth System Sciences, 17, 2013.

Tiwari, V. M., Wahr, J., and Swenson, S.: Dwindling groundwater resources in northern India, from satellite gravity observations, Geophysical Research Letters, 36, L18 401, doi:10.1029/2009GL039401, http://doi.wiley.com/10.1029/2009GL039401, 2009.

Vaidyanathan, A., for Science, C., and Environment (New Delhi, I.: Tanks of South India, Centre for Science and Environment, https://books.google.com/books?id=zHWOGQAACAAJ, 2001.

Van Meter, K. J., Basu, N. B., Tate, E., and Wyckoff, J.: Monsoon harvests: The living legacies of rainwater harvesting systems in South India, Environmental Science and Technology, 48, 4217–4225, doi:10.1021/es4040182, http://pubs.acs.org/doi/abs/10.1021/es4040182, 2014.

Van Meter, K. J., Basu, N. B., McLaughlin, D. L., and Steiff, M.: The socio-ecohydrology of rainwater harvesting in India: understanding water storage and release dynamics at tank and catchment scales, Hydrology and Earth System Sciences Discussions, 20, 2629–2647, doi:10.5194/hessd-12-12121-2015, http://www.hydrol-earth-syst-sci-discuss.net/12/12121/2015/, 2016.

Vogel, R. M., Lall, U., Cai, X., Rajagopalan, B., Weiskel, P. K., Hooper, R. P., and Matalas, N. C.: Hydrology: The interdisciplinary science of water, Water Resources Research, 51, 4409–4430, doi:10.1002/2015WR017049, http://onlinelibrary.wiley.com/doi/10.1002/2015WR017049/full, 2015.

Vörösmarty, C. J., McIntyre, P. B., Gessner, M. O., Dudgeon, D., Prusevich, a., Green, P., Glidden, S., Bunn, S. E., Sullivan, C. a., Liermann, C. R., and Davies, P. M.: Global threats to human water security and river biodiversity., Nature, 467, 555–561, doi:10.1038/nature09549, http://www.ncbi.nlm.nih.gov/pubmed/20882010, 2010.

Wada, Y., Van Beek, L. P. H., and Bierkens, M. F. P.: Nonsustainable groundwater sustaining irrigation: A global assessment, Water Resources Research, 48, doi:10.1029/2011WR010562, 2012.

Whitlock, C. H., Poole, L. R., Usry, J. W., Houghton, W. M., Witte, W. G., Morris, W. D., and Gurganus, E. a.: Comparison of reflectance with backscatter and absorption parameters for turbid waters., Applied optics, 20, 517–522, doi:10.1364/AO.20.000517, 1981.

Wickham, H.: ggplot2: Elegant Graphics for Data Analysis, Springer-Verlag New York, http://had.co.nz/ggplot2/book, 2009.

Womack, J. M. et al.: Evaluation of the hydrologic effects of stock ponds on a prairie watershed, Ph.D. thesis, Montana State University-Bozeman, College of Engineering, 2012.

Xiankun, Y.: Reservoir delineation and cumulative impacts assessment in large river basins: A case study of the Yangtze River Basin, Ph.D. thesis, 2014.

Xu, Y., Fu, B., and He, C.: Assessing the hydrological effect of the check dams in the Loess Plateau, China, by model simulations, Hydrology and Earth System Sciences, 17, 2185–2193, 2013.

Zhu, Z. and Woodcock, C. E.: Object-based cloud and cloud shadow detection in Landsat imagery, Remote Sensing of Environment, 118, 83–94, doi:10.1016/j.rse.2011.10.028, http://linkinghub.elsevier.com/retrieve/pii/S0034425711003853, 2012.

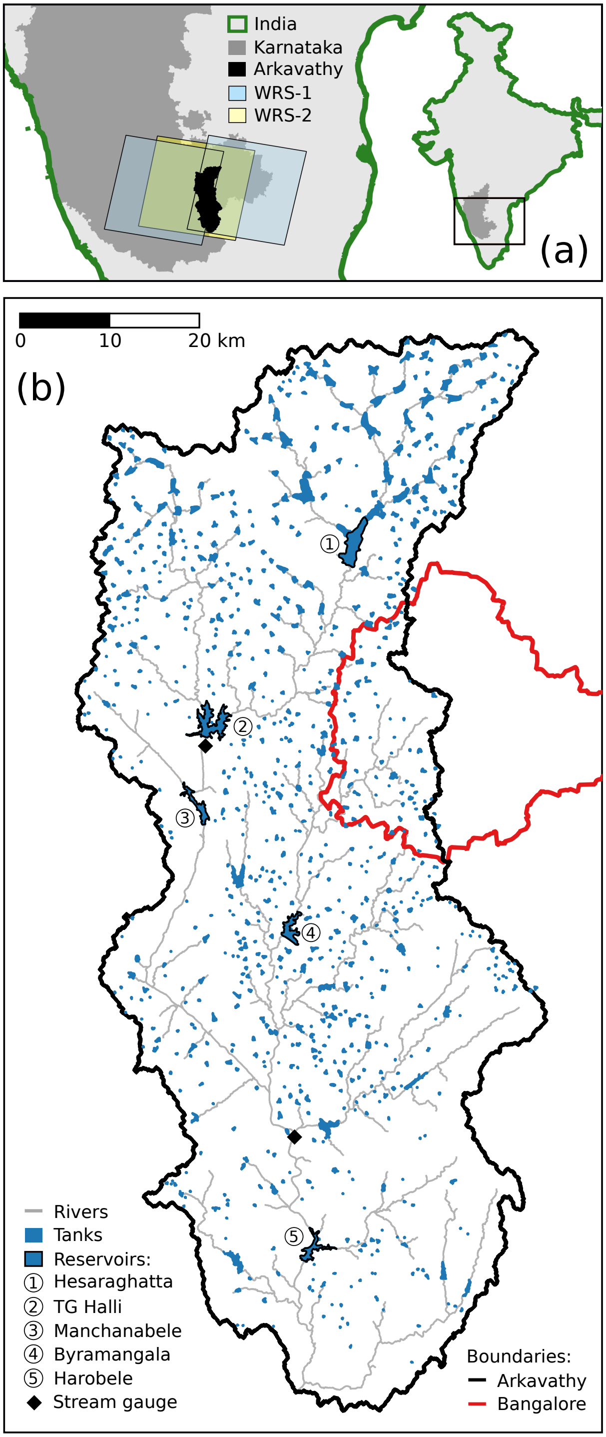

Figure 1. Site map. (a) Location of the Arkavathy watershed within the state of Karnataka, India, and scene boundaries for Landsat 1–3 (WRS-1) and Landsat 4–8 (WRS-2). (b) Map of the watershed including tanks, reservoirs including the stream gauge locations, river network, and municipal boundary of Bangalore. Lower-order streams and a number of small, generally dry tanks are excluded.

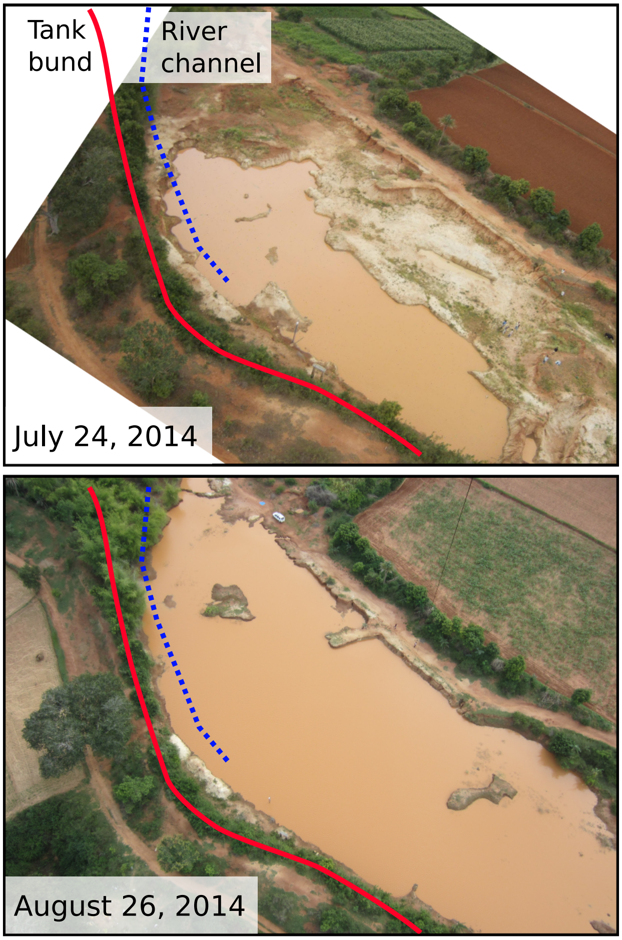

Figure 2. Aerial photos of a small tank containing turbid water in the Arkavathy watershed before and after runoff events in August 2014. The tank receives water from the channel and directly from adjacent agricultural plots, and water extent increases with storage.

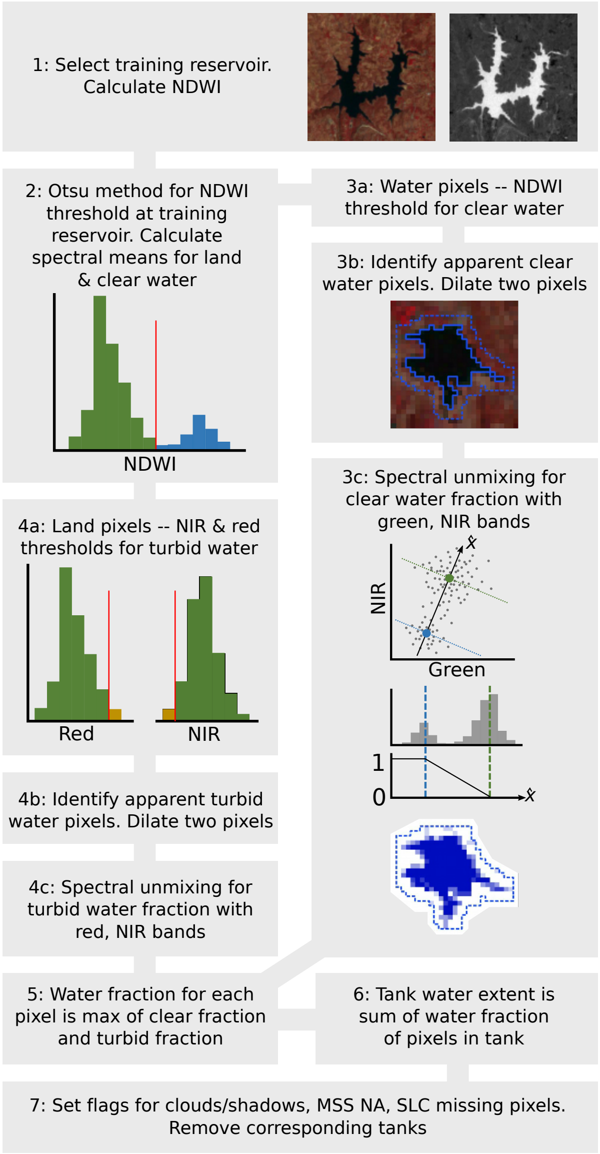

Figure 3. Flowchart of classification method. In Steps 3 and 4, clear water fraction and turbid water fraction are each calculated for all pixels in the image before they are combined into water fraction in Step 5. Color images are from Landsat, with red, green, and blue in the image corresponding to NIR, Red, and Green bands from Landsat TM.

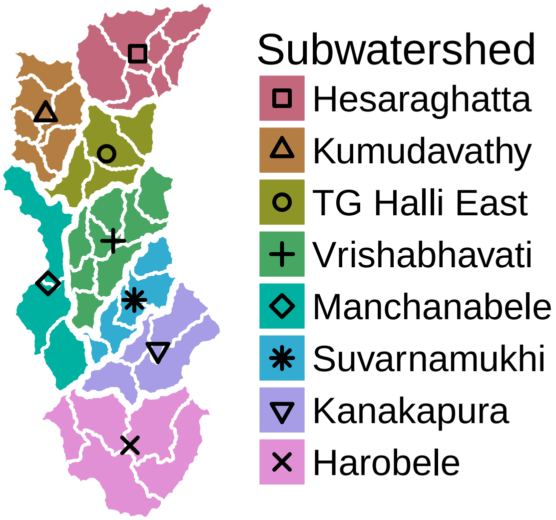

Figure 4. Subwatersheds and tank cluster watersheds. Each tank cluster contained at least 15 tanks.

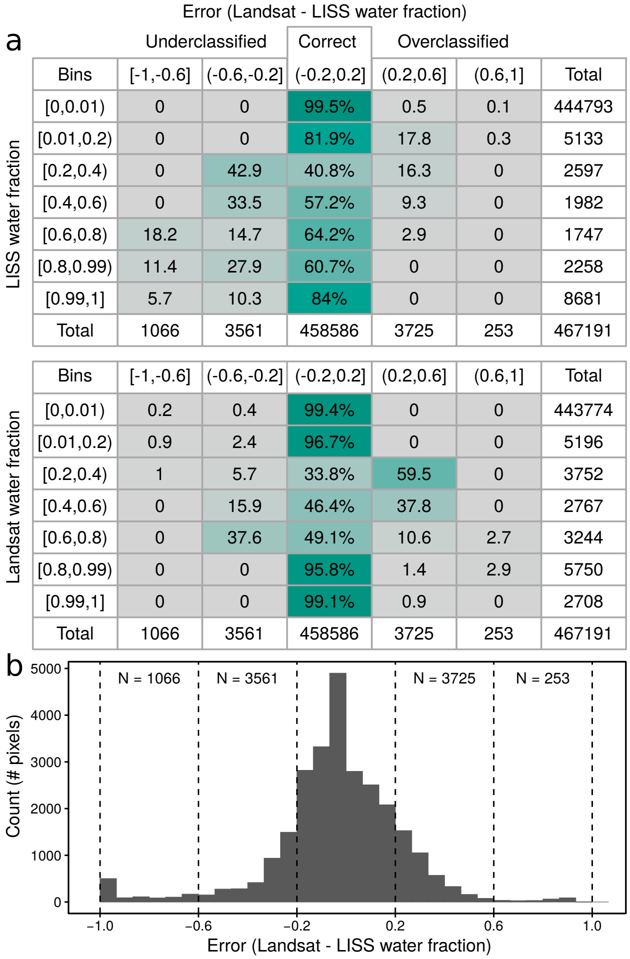

Error (Landsat - LISS water fraction)

		Underclassified		Correct	Overclassified		
	Bins	[-1,-0.6]	(-0.6,-0.2]	(-0.2,0.2]	(0.2,0.6]	(0.6,1]	Total
LISS water fraction	[0,0.01)	0	0	99.5%	0.5	0.1	444793
	[0.01,0.2)	0	0	81.9%	17.8	0.3	5133
	[0.2,0.4)	0	42.9	40.8%	16.3	0	2597
	[0.4,0.6)	0	33.5	57.2%	9.3	0	1982
	[0.6,0.8)	18.2	14.7	64.2%	2.9	0	1747
	[0.8,0.99)	11.4	27.9	60.7%	0	0	2258
	[0.99,1]	5.7	10.3	84%	0	0	8681
	Total	1066	3561	458586	3725	253	467191

	Bins	[-1,-0.6]	(-0.6,-0.2]	(-0.2,0.2]	(0.2,0.6]	(0.6,1]	Total
Landsat water fraction	[0,0.01)	0.2	0.4	99.4%	0	0	443774
	[0.01,0.2)	0.9	2.4	96.7%	0	0	5196
	[0.2,0.4)	1	5.7	33.8%	59.5	0	3752
	[0.4,0.6)	0	15.9	46.4%	37.8	0	2767
	[0.6,0.8)	0	37.6	49.1%	10.6	2.7	3244
	[0.8,0.99)	0	0	95.8%	1.4	2.9	5750
	[0.99,1]	0	0	99.1%	0.9	0	2708
	Total	1066	3561	458586	3725	253	467191

Figure 5. (a) Pixel-level producer and consumer accuracy tables, given by percent of pixels within a given error bin. Pixels are grouped into rows by the producer or consumer water fraction and then binned into columns by the error (Landsat - LISS water fraction). The center column shows the percentage of pixels that were correctly classified, with error between -0.2 and 0.2. (b) Histogram of non-zero classification errors (excluding pixels where the error was zero).

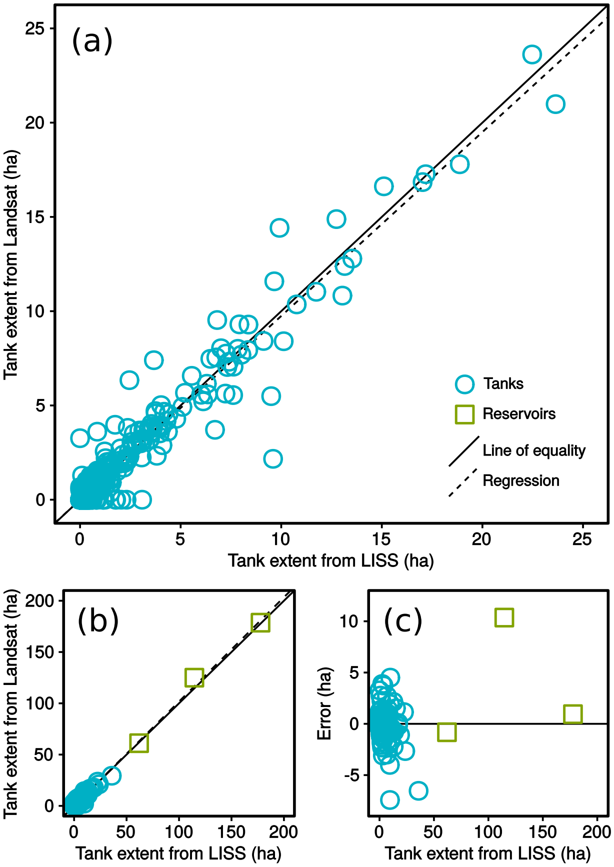

Figure 6. Comparison of Landsat and reference (LISS) classification from February 2014 images. (a) Water extent in tanks less than 25 ha. (b) Water extent in all tanks and reservoirs. (c) Error in the Landsat classification for tanks and reservoirs. Relative error decreases with increasing tank size. Only three of the five reservoirs are included because the LISS image excluded the Harobele reservoir and there was considerable change in an algae bloom in the Byramangala reservoir in the time between the acquisition of the LISS and Landsat images.

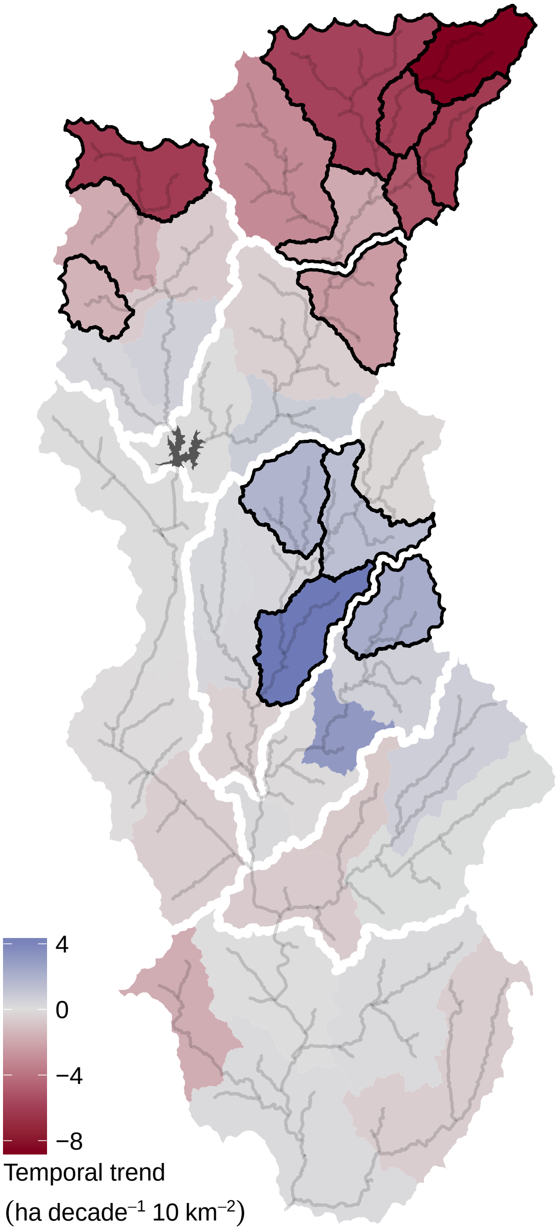

Figure 7. Trends in cluster water extent, 1973–2010, given as change in water surface area (ha) per decade per 10 km^{2} of watershed area. White space indicates subwatershed boundaries, and black lines indicate statistical significance of the cluster trend.

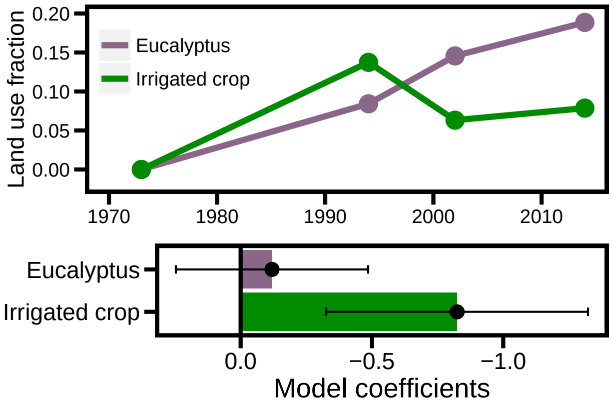

Figure 8. Agricultural land use and hydrological change. (Top) Land use fraction of *Eucalyptus* plantations and irrigated crops in four land use maps. (Bottom) Model coefficients relating hydrological change to *Eucalyptus* and irrigated crops based from the multivariate linear regression. Horizontal lines indicate 95% confidence intervals.